

NEW INSIGHTS INTO SHIP-FLOODWATER-SEA DYNAMICS

Luca LETIZIA, Safety at Sea Ltd., Glasgow, (Scotland), Dracos VASSALOS, The Ship Stability Research Centre, Department of Naval Architecture and Marine Engineering, the Universities of Glasgow and Strathclyde, (Scotland)
and Andrzej JASIONOWSKI, Safety at Sea Ltd., Glasgow, (Scotland)

Abstract

This paper aims to clarify a number of issues concerning the dynamics of a damaged ship, interpreting the results of recent towing tank tests by means of a simplified linear model with two degrees of freedom. In this sense, this work can be seen as the natural evolution of the extensive body of work in this field undertaken by the SSRC during a long series of large research projects, including the Joint North West European Project [2], the MCA funded Time Based Survival Criteria of Passenger Ro-Ro Vessels, Phase 1 and 2 [3] and, above all, the Fifth EC Framework RTD projects HARDER and NEREUS [1], during which the experimental evidence presented in this paper was collected.

1. INTRODUCTION

During previous research, a large discrepancy was observed between the RAO curves produced by numerical simulations of the dynamic behaviour of damaged ships and those extracted from the results of physical damage survivability model tests. Specifically, the position of the experimental RAO peak seemed to be shifted towards the lower frequency end, and its size was significantly smaller than the numerical counterpart. Initially, it was thought that this was caused by an alteration of the radiated and diffracted wave, causing a significant increase of added inertia and roll damping. From this first hypothesis stemmed a series of research activities and an extensive experimental programme, all aiming to verify and quantify this assertion.

Following more systematic testing, a second peak was observed, shifted towards the higher frequency end [1]. This second peak clearly

pointed towards more complex dynamics than a simple change in the basic ship hydrodynamics. In order to reproduce this effect, a simplified version of water sloshing dynamics was introduced in the numerical simulation. Unfortunately, this improvement of the model has only partially successfully reproduced the observed RAO (see Figure 7 and Figure 6). In parallel with this development, a more complex numerical model was created, which uses viscous CFD techniques to simulate the floodwater dynamics [4]. This second type of simulations was extremely useful in clarifying a number of phenomena that are not correctly reproduced in the simpler numerical models, nevertheless, to date only a partial set of results is available to assess the capability of viscous CFD to reproduce the double peaked RAO observed. From the few points available, it seems that although the position of the lower frequency peak is reasonably well captured, its size is still not correctly replicated (see Figure 9).



All of the above called for a fundamental rethinking of the damaged ship dynamics. Amongst the many questions raised, there was the issue concerning the effect of inflow/outflow through the damage opening over the ship hydrodynamic coefficients (radiation damping and added inertia). Another point concerned the qualification of the main differences between the effects of floodwater dynamics as normally modelled for classic sloshing in tanks (flooded compartment segregated from the sea) and those that are characteristic of the more complex damaged compartment case (even in cases where the floodwater inertia variation in time could safely be considered small).

In order to answer these questions, during the last series of tests within NEREUS, RAO curves for a sample ship were carefully measured experimentally in three conditions, namely:

- Intact condition
- Damage condition
- Intact condition with an amount of floodwater equivalent to the one present in the damaged compartment (this will be referred to as the “trapped water” condition)

The comparison of these three RAOs clearly and unequivocally demonstrated that damaged ship dynamics are fundamentally different from those of an intact ship with an amount of water sloshing in one of its compartments (see Figure 5). The variation of the RAO curves, though, did not answer specific questions, such as: what aspect of dynamics and which parameters are dominant contributors in making the damaged ship RAO so different from that of the “trapped water” counterpart? To answer these questions and gain new insights into the more fundamental ones mentioned above, the authors undertook to analyse the results of this last series of model tests, with the aid of classic

linear theory of a simple two degrees of freedom mechanical oscillator model.

2. EXPERIMENTAL EVIDENCE

This section details the model experiments carried out on behalf of the NEREUS project by the Ship Stability Research Centre of the Universities of Glasgow and Strathclyde at the Ship Survivability Test Centre in Dumbarton (Denny Tank). The main purpose of the model experiments was to investigate the damage survivability of the passenger/Ro-Ro vessel ‘Color Innovator’ designed by Flensburger Schiffbau-Gesellschaft as part of the project. The model experiments were performed adopting the Model Test Method prescribed by the SOLAS 1995 Conference Resolution 14, ‘Regional Agreement on Specific Stability Requirements for Ro-Ro Passenger Ships’, and the Guidance Notes for a Uniform Test Procedure issued by the UK Maritime and Coastguard Agency only as general guidelines.

The main bulk of these tests aimed to establish the capsize boundary of the subject vessel. Nevertheless, additional tests were also performed in order to ascertain possible differences in the static stability characteristics of the model compared to those assumed for the vessel. Also, ad-hoc tests were run for the model to establish roll RAO curves for the ship in a number of conditions (intact, damaged and with water trapped in the compartments under the vehicle deck). In the following a brief account is given only of the latter part.

2.1. Details of the vessel

‘Color Innovator’ is a passenger/Ro-Ro vessel to be operated without restrictions, i.e. with a required significant wave height (H_s) of 4.00 m. The general particulars of the vessel, both full scale and model scale, are shown in Table

1. The model was constructed at a scale of 1:40.

Table 1: General Particulars

Dimension	Full Scale	Model Scale
LOA	201.623 m	5040.6 mm
LBP	189.100 m	4727.5 mm
B	29.900 m	747.5 mm
DCARDECK	10.000 m	250.0 mm
T	6.700 m	167.5 mm
Displacement (even keel)	20828.1 tonnes	325.44 kg

The worst damage case was selected according to the calculations carried out by FSG and corresponds to the worse SEM [2] case (i.e. the damage case with the lowest survivable H_s as estimated by this method). This is damage case 96...124, as shown in Figure 1, with a standard damage opening centred on frame 113. The same set of calculations show that this case is also the worst case as specified by the Appendix of Resolution 14 of the 1995 SOLAS Conference Model Test Method, i.e. the damage which gives the least area under the residual stability curve. Loading conditions for damage case 96...124 are shown in Table 2. Note that the target intact GM is 2.229 m.

Inclining tests were performed following standard practice for the intact ship as well as for the damage configurations. The results are shown in Table 3 to Table 5. Note that the target GM in Table 4 is that calculated by FSG. According to FSG damage stability calculations, the heel angle at equilibrium should have been equal to 2.242. Table 4 shows that neither the measured damage GM nor the angle of heel at equilibrium matched the FSG estimates.

Table 5 shows results for the intact model with an amount of trapped water in the compartments below the vehicle deck equal to that which would be there if the ship were damaged (trapped water condition).

Since neither the angle of heel at equilibrium nor the measured damage GM matched the

damage stability results provided by FSG, a series of tests to measure the intact and damage GZ curve were carried out for the intact ship and the various damage configurations. These measurements were taken simply by shifting ballast weights transversally and recording heeling moments (weight x distance) and the ensuing heel angle. Figure 2 and Figure 3 show the results of this exercise with numerical values obtained by SSRC using the dynamic survivability software PROTEUS 3 and the hydrostatic suite NAPA, together with the data provided by FSG.

Table 2: Intact Vessel Loading Condition

Item	Full Scale	Model Scale	
		Calculated	Measured
Displacement/ Weight	20828.10 tonnes (Fresh water)	325.44 kg (Fresh water)	325.40 kg (Fresh water)
Draught AP	6.70 m	167.5 mm	**
Draught 0.25LBP	6.70 m	167.5 mm	167.0 mm
Draught Amidships	6.70 m	167.5 mm	167.0 mm
Draught FP	6.70 m	167.5 mm	167.0 mm
Trim	Even keel	Even keel	Even keel

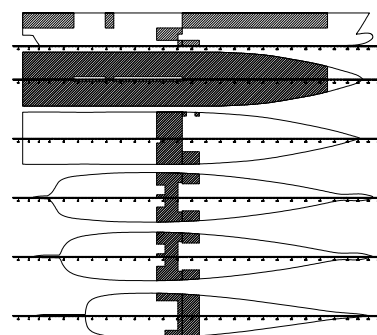


Figure 1: Spaces open to flooding

Table 3: Inclining test results for the intact model

** Due to the shape of the model it was not possible to measure the draft at the AP



Item	Full Scale	Model Scale
Displacement	20825.6 tonnes	325.4 kg
<i>d</i>	16.520 m	413.00 mm
<i>w</i>	70.272 kg	1.098 kg
Target GM	2.229 m	55.70 mm
Measured angle of inclination (Φ)	1.441 deg.	1.441 deg.
Measured GM	2.215 m	55.38 mm

Table 4: Inclining test results for the damaged model

Item	Full Scale	Model Scale
Displacement	20825.6 tonnes	325.4 kg
<i>D</i>	4.960 m	124.00 mm
<i>W</i>	70.272 kg	1.098 kg
Target GM	1.745 m	43.625 mm
Measured angle of inclination (Φ)	0.16±0.652 deg.	0.16±0.652 deg.
Measured GM	1.470 m	36.756 mm

Table 5: Inclining test results for the model with trapped water

Item	Full Scale	Model Scale
Displacement	20825.6 tonnes	325.4 kg
<i>d</i>	4.960 m	124.00 mm
<i>w</i>	70.272 kg	1.098 kg
Target GM	1.745 m	43.625 mm
Measured angle of inclination (Φ)	0.12±0.634 deg.	0.12±0.634 deg.
Measured GM	1.513 m	37.817 mm

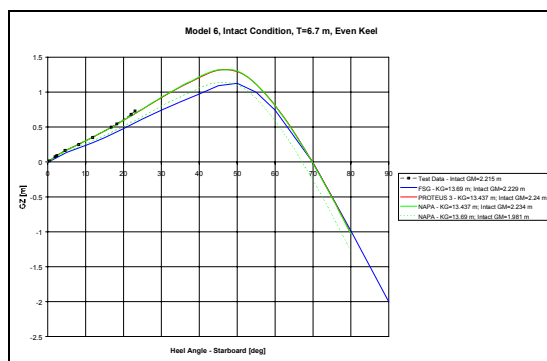


Figure 2: Intact GZ curve comparison.

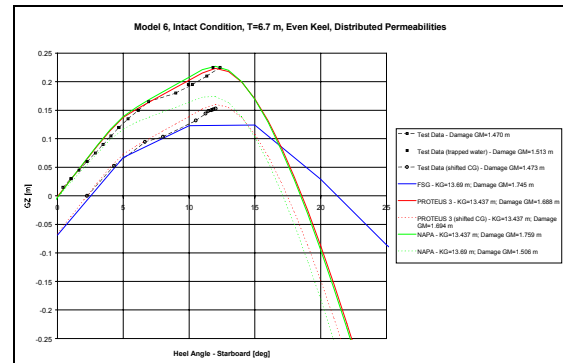


Figure 3: Damage GZ curve comparison

Figure 2 shows the intact GZ curve for the model as obtained experimentally, compared with four numerical estimates. The following observations can be made:

- FSG intact stability does not match either in terms of initial GM or for large heel angles
- PROTEUS 3 and NAPA match very well with the experimental evidence, provided one assumes a value of KG such that the correct initial GM value (2.229) is preserved. This corresponds to a KG value of 13.437 m (rather than 13.69 m as was initially suggested)

Figure 3 shows the damage GZ curves for the model as obtained experimentally for three damage configurations (base, shifted CG and trapped water – the shifted CG configuration is not relevant to the contents of this paper). These are compared with five numerical estimates, namely:

- The damage GZ curve provided by FSG
- The damage GZ curve calculated using PROTEUS 3 with a KG value of 13.437 m (equivalent to the correct value of intact GM of 2.229 m)
- The damage GZ curve calculated using PROTEUS 3 with a KG value of 13.437 m and a shift of CG such that an initial angle of heel of 2.24 degrees is obtained
- The damage GZ curve calculated using NAPA with a KG value of 13.437 m

(equivalent to the correct value of intact GM of 2.229 m)

- The damage GZ curve calculated using NAPA with a KG value of 13.69 m (as suggested by FSG)

The following observations can be made:

- The experimental curve obtained for the base damage case compares well with that obtained for the model with trapped water. The two curves start diverging slightly at higher heel angles when floodwater starts flooding the vehicle deck in the first case but not in the second. The equivalence of these hydrostatic results should be born in mind when comparing the RAO curves measured for these two damage configurations
- The experimental curves compare reasonably well with the numerical estimates obtained using PROTEUS 3 and NAPA for the right value of KG (13.437 m), although the effect of finite wall thickness and permeability blocks can be observed in the fact that the numerical curves are generally higher than the experimental ones (effect of permeability blocks), whilst the experimental curves show an inflexion for higher heel angles that cannot be observed in the numerical ones (finite wall thickness effect). Damage GM values calculated numerically are generally consistent with each other but noticeably different from those measured experimentally.

Free roll tests in calm water were carried out in order to estimate the natural roll period (T_n). The roll radius of gyration can then be approximately determined using the following expression:

$$K_{xx} = \frac{T_n \sqrt{gGM}}{2\pi}$$

A summary of the intact free rolling test is given in Table 6, while the full scale time history of the test is given in Figure 14.

Table 6: Intact free rolling test results

Item	Full Scale	Model Scale
Measured GM	2.215 m	55.38 mm
Measured natural roll period	14.365 sec	2.271 sec
Roll radius of gyration (K_{xx})	10.658 m	266.4 mm
B	29.900 m	747.5 mm
K_{xx}/B	0.356	0.356

Note that free roll oscillation tests were also performed for the base damage configuration ($KG = 13.437$ m) and for the trapped water configuration.

2.2. Test programme and results

The test section of the sea-keeping tank is 90 m long, 7.0 m wide and 2.7 m deep with a wave maker at one end and a beach at the other. The wave maker has 5 independent flaps capable of generating regular and irregular waves using in-house software. Motions were measured by using an infrared camera system, a sophisticated non-contact motion measuring system available at the Centre. This system can measure with extreme accuracy the motions of a free model in six-degrees-of-freedom. Roll and pitch motions are also measured using an electronic inclinometer, attached to the centre of gravity of the vessel, to readily provide motion records during the experiments. Waves are measured by means of wave probes.

The model is initially positioned 20 m away from the wave maker. When the set-up is ready, random wave realisations are generated by and sent to the wave maker. The wave train is ramped up slowly to avoid serious initial transient motion. It is important to note that this implies that the RAO curves derived were measured on a model which was not restrained in any way at all. Regular waves were run for

very small values of wave height (0.5 or 1.0 m depending on the frequency) to ensure that the oscillations would stay in the linear range of the GZ curves. Frequency settings were chosen so that a denser definition of the RAO curve would be available to properly define the peaks.

The intact, base damage and trapped water configurations were all tested in regular waves to estimate standard RAO curves. The summary of the results is given in Figure 5. Figure 4 shows the results collected for PRR1 during the model tests run for project HARDER. It is interesting to note that the double peaked RAO curve already observed for the PRR1 damage case, is also captured for the ‘Color Innovator’. It is also interesting to note (see Figure 1) that this double peak is equally present in the trapped water case but that the peaks in the latter case are shifted towards the lower frequency range. Also note that the trapped water case higher peak is higher than the open flooding counterpart.

Figure 6 to Figure 9 show the results of numerical simulations (SSRC PROTEUS and WS Atkins viscous CFD code NEREID) run for the ship PRR1, compared to the experimental results. It is interesting to note that although the nature of the curve (double peak) is captured by PROTEUS, the position and size of the peaks is not quite correct. In the case of NEREID, the position of the lower frequency peak seems well captured but its size is still elusive.

In general, it is clear from these results that damaged ship RAO curves are significantly smaller than the original intact ship RAO (damped roll motion) as a result of ship-floodwater-sea dynamics. It is also clear that trapping floodwater in the compartments below the vehicle deck (as some numerical methods assume) alters significantly the nature of the damaged vessel RAO curve. In particular, whilst both peaks are shifted towards lower

frequencies, the high frequency peak is significantly higher than both free flooding peaks.

3. LINEAR THEORY MODEL

In order to interpret the experimental results described above, a simple two degrees of freedom model was adopted. Figure 10 shows a schematic of this system, illustrating the meaning of each of the parameters used in the equations of motion (Eq. 1). The latter can be solved analytically in vectorial (complex) form, assuming an excitation of the form given in Equation 2, to derive expressions for the RAO of the motion of both masses.

$$\begin{cases} m_1 \ddot{q}_1 = f_1(t) - c_1 \dot{q}_1 - k_1 q_1 - c_2 (\dot{q}_1 - \dot{q}_2) - k_2 (q_1 - q_2) \\ m_2 \ddot{q}_2 = -c_2 (\dot{q}_2 - \dot{q}_1) - k_2 (q_2 - q_1) \end{cases} \quad \text{Eq. 1}$$

where,

$$f_1(t) = F_1 e^{i\omega t} \quad \text{Equation 2}$$

In order to draw a parallel between this simple system and the case of a ship with a flooded compartment, each of the parameters given above need to be associated with a quantity representative of the ship and floodwater dynamics. As far as m_1 , c_1 , k_1 , f_1 and q_1 are concerned, the choice is fairly straightforward. The following is assumed:

$$m_1 \quad \text{Intact ship virtual inertia in roll} \quad m_1 = \Delta_s K_{xxs}^2$$

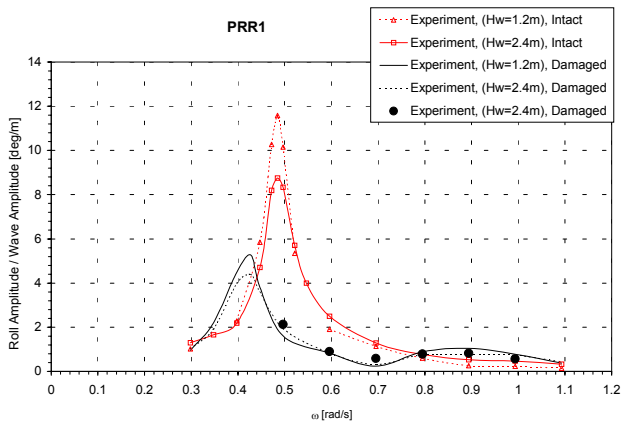


Figure 4: PRR1 roll response per wave amplitude curves (experimental)

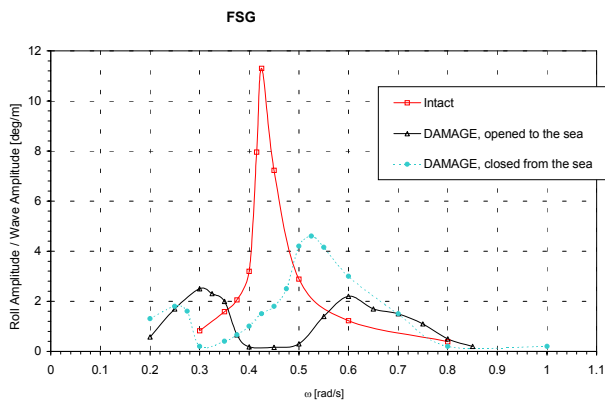


Figure 5: Color Innovator roll response per wave amplitude curves (experimental)

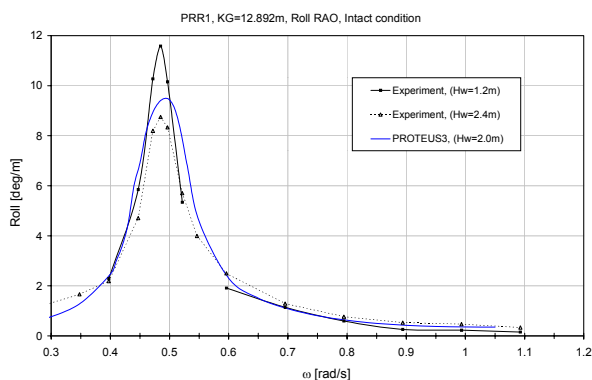


Figure 6: PRR1 roll response per wave amplitude, comparison between experiment and numerical simulations (PROTEUS3), intact condition

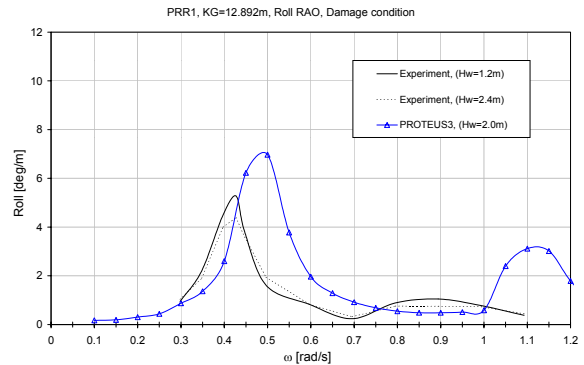


Figure 7: PRR1 roll response per wave amplitude, comparison between experiment and numerical simulations (PROTEUS3), damage condition

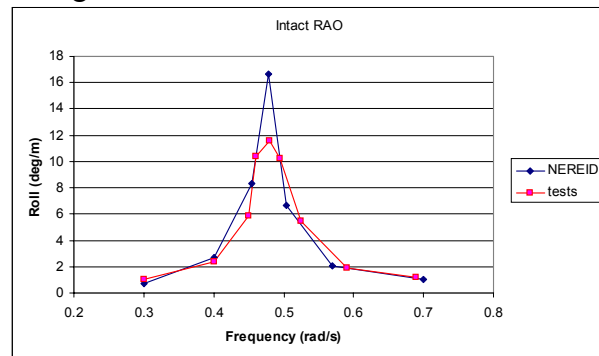


Figure 8: PRR1 roll response per wave amplitude, comparison between experiment and numerical simulations (Viscous CFD code NEREID), intact condition

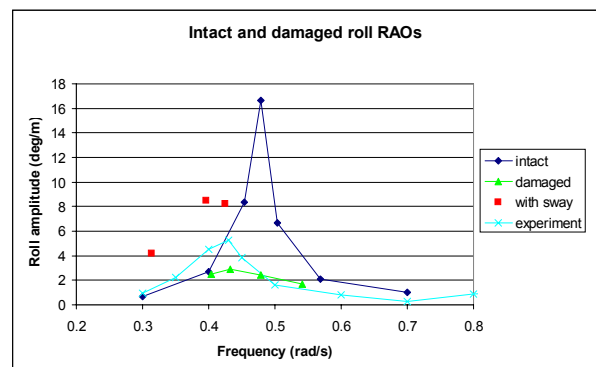


Figure 9: PRR1 roll response per wave amplitude, comparison between experiment and numerical simulations (Viscous CFD code NEREID), damage condition

$$\Delta_d KG_d = \Delta_s KG_s + \Delta_t KG_t$$

and

$$\Delta_d = \Delta_s + \Delta_t$$

If k_2 is infinite, it must be (see Figure 10):

$$m_{1\text{equivalent frozen}} = m_1 + m_2$$

therefore

$$m_2 = \Delta_t K_{\text{xxt}}^2 + \Delta_t \overline{G_s G_t}^2$$

This value for m_2 is, of course, only a reference value and is expected it to change significantly whenever the “frozen floodwater” condition is not met. Nevertheless, it offers a good yardstick against which the effect of floodwater dynamics on the internal inertia of the system can be compared.

As far as k_2 is concerned, its reference value can be defined by looking at another limit case: the familiar zero-frequency motion assumed by all hydrostatic analysis. In this case the surface of the floodwater would always be parallel to the horizon and thus q_2 would always be zero. Examining Figure 10, one quickly realises that

$$k_{1\text{equivalent trapped}} = k_1 + k_2$$

Now, inspecting Figure 11 and bearing in mind that the weight of the floodwater according to the linearity assumption assumed here can be seen as an equivalent weight applied to the metacentre of the flooded compartment M_t , it is easy to demonstrate that:

$$\begin{aligned} k_{1\text{equivalent trapped}} &= g \left(\overline{KM_d} - \overline{KG_d} - \rho \frac{I_{\text{xxt}}}{\Delta_d} \right) \Delta_d \\ &= g \left(\frac{1}{\Delta_d} \left(\Delta_s^2 \overline{G_s M_d} + (2\Delta_t \Delta_s + \Delta_t^2) \overline{G_t M_d} \right) - \rho I_{\text{xxt}} \right) \end{aligned}$$

where I_{xxt} is the moment of the free surface area in the compartment. The value of k_2 will therefore be:

$$k_2 = g \left(\frac{1}{\Delta_d} \left(\Delta_s^2 \overline{G_s M_d} + (2\Delta_t \Delta_s + \Delta_t^2) \overline{G_t M_d} \right) - \rho I_{\text{xxt}} - \Delta_s \overline{G_s M_s} \right) \quad \text{Eq. 3}$$

Note that this value of k_2 takes into account all the variations of ship hydrostatics that a free surface/damage causes and which are familiar to all naval architects. A way to see this is to simplify the above equation for k_2 , considering Δ_t small enough to be negligible. In that case, k_2 reduces to:

$$k_2 = g \left(\overline{\Delta_s M_s M_d} - \rho I_{\text{xxt}} \right)$$

which is the variation of metacentric height due to the new immersion, minus the free surface correction.

Eq. 3 will be used as a reference for the internal restoring, although it is to be expected that due to floodwater dynamics, its value for finite frequency motion will be significantly different from this theoretical limit.

4. DATA ANALYSIS

The main aim of this exercise is to try and quantify the effect of flooding through a damage opening on the ship behaviour, providing an insight on which proportion of this effect can be associated with a change in floodwater dynamics (m_2 , c_2 and k_2) and which can be associated with a change to the ship hydrodynamics (m_1 and c_1). It is to be noted that, having chosen to include all variation of the ship restoring in k_2 , k_1 we has been assumed to be invariant.

$$\begin{aligned} k_1 &= g \Delta_s \overline{G_s M_s}, \quad \overline{G_s M_s} = 2.215 \text{ m}, \\ \Delta_s &= 20825600 \text{ kg} \end{aligned}$$

Conversely, possible variations of m_1 and c_1 will be attempted, since these quantities are representative of the ship virtual inertia and external roll damping.

In order to achieve the above, an attempt will be made to match the three RAO curves in Figure 5 by tuning the simple two degrees of freedom model of Figure 10. Following this, the ensuing values of m_1 , m_2 , c_1 , c_2 and k_2 will be compared with their theoretical reference values, as derived above.

4.1. Intact ship

The intact ship RAO curve can be easily matched by assuming the following:

$$m_1 = \Delta_s K_{xxs}^2, K_{xxs} = 11.1 m$$

$$m_2 = 0.0$$

$$c_1 = 1.01E8$$

$$k_2 = 0.0$$

Note that to match the position of the RAO peak, the assumed value of K_{xxs} is slightly higher than the one measured in the tank. This is likely to be simply due to experimental error. The value of c_1 was tuned to match the peak height and confirmed by matching the experimental roll decay curve (see Figure 14 and Figure 13). Also note that m_1 and k_1 need to be zero (the ship is intact).

The resulting curve (red curve in Figure 12) matches fairly well the experimental one (red curve in Figure 5), in the sense that both position and height of the peak are accurately captured. It is to be noted, though, that the linear system RAO width at the base of the peak is somewhat broader than the experimental one. Also, whilst the experimental curve tends to zero for increasing frequency values, the linear system does not. The latter effect is due to having assumed

excitation amplitude constant with frequency for the linear system, whilst wave excitation amplitude decreases as the frequency increases.

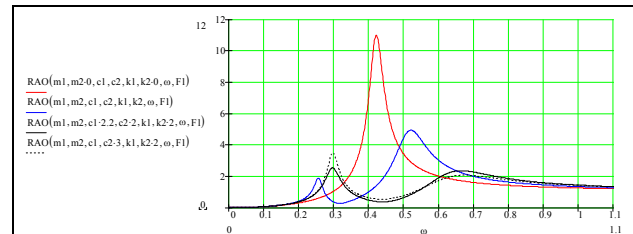


Figure 12: Color Innovator roll response per wave amplitude curves (linear model)

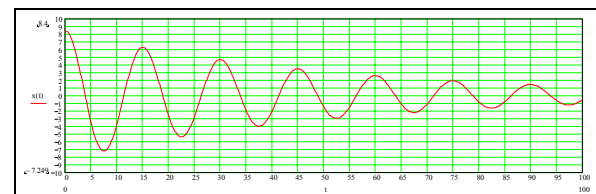


Figure 13: Color Innovator roll decay curve (linear model)

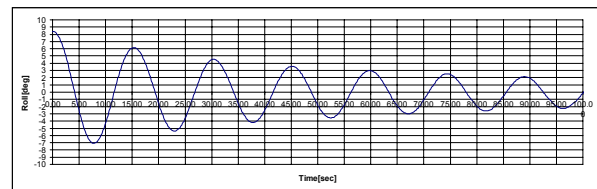


Figure 14: Color Innovator roll decay curve (experimental)

4.2. Trapped water

Before explaining how the trapped water RAO was matched (compare the blue curves in Figure 5 and Figure 12), it might be worth mentioning what the effect of the variation of the six system parameters m_1 , m_2 , c_1 , c_2 , k_1 and k_2 is on the RAO curve. This is briefly reported in Table 7.

Table 7: Parametric variation effects on the linear system RAO

Parameter	Principal effects of an increase in the value of the parameter
m_1	- Shifts both peaks to lower frequency end - Raises lower frequency peak height and lowers higher frequency peak height
m_2	- Shifts both peaks to lower frequency end - Lowers lower frequency peak height and raises higher frequency peak height
c_1	- Lowers the whole curve proportionally
c_2	- Lowers the height of both peaks proportionally and raises the curve between the peaks
k_1	- Shifts both peaks to higher frequency end - Lowers lower frequency peak height and raises higher frequency peak height
k_2	- Shifts both peaks to higher frequency end - Raises lower frequency peak height and lowers higher frequency peak height

Clearly, the lower frequency peak is associated with mass m_1 (ship) whilst the higher frequency peak is associated with mass m_2 (floodwater). Furthermore, note that the damping coefficients c_1 and c_2 do not significantly vary the position of the peaks (natural frequencies of the system) nor change their relative height (ratio between the height of the peaks).

One corollary of the above is that in order to vary the distance between the two peaks keeping control on the relative height, one must vary k_2 (having assumed k_1 invariant) since a combination of m_1 and m_2 would necessarily introduce a variation in the relative peak height for any variation of the inter-peak distance. Furthermore, since c_1 and c_2 do not affect significantly the position of the peaks, one is left with three parameters (two peak positions and relative height) and three unknowns (m_1 , m_2 and k_2).

Following the above, one would expect having to change all three parameters m_1 , m_2 and k_2 to match the trapped water curve. In fact, this is not the case, since it is possible to do so simply by assuming the following:

$$m_1 = \Delta_s K_{xxs}^2, K_{xxs} = 11.1 m$$

$$m_2 = \Delta_t K_{xxt}^2 + \Delta_t \overline{G_s G_t}^2, K_{xxt} = 21.5 m,$$

$$\Delta_t = 2613600 kg, \overline{G_s G_t} = 9.507 m$$

$$c_1 = 1.01E8$$

$$c_2 = 7.07E7$$

$$k_2 = 1.838 k_{2 \text{ reference}}$$

where $k_{2 \text{ reference}}$ is as given from Eq. 3 and was calculated from hydrostatics, as were the values of Δ_t and $G_s G_t$. K_{xxt} was instead tuned to suit.

Note that m_1 has the same value as that assumed to match the intact ship RAO. This means that the increase in draught due to the added floodwater has not changed the added inertia of the ship significantly. Also note that c_1 has not been varied (a variation in c_1 would imply a poor match of the two RAO curves between the peaks, if the values of the peaks is well matched) indicating that the ship external damping has not changed either. In other words, this means that all of the differences between the RAO for the intact ship and the trapped water conditions are due to internal floodwater dynamics.

It is interesting to note that both values of floodwater inertia and restoring are much higher than their reference values. In particular, the radius of gyration of the floodwater is about 0.74 times the breadth of the damaged compartment. This alone puts the assumption that floodwater can be approximated by point masses into perspective. Also interesting is to note that the value of the internal damping is of the same order of magnitude as that of the external damping (as one might have expected).

4.3.Damaged ship

In order to match the main characteristics of the damaged ship RAO (compare the solid black curves in Figure 5 and Figure 12), one is forced to change more than simply m_2 , c_2 and

k_2 . The best match varying only the floodwater parameters is shown in Figure 12 as a dotted black line. This is achieved by increasing the value of internal damping of the corresponding trapped water case by a factor of three and doubling the internal stiffness. Clearly, although the position of the two peaks and the height of the higher frequency peak for the linear RAO are satisfactory (compatibly with the non-linear shape of the experimental curve), the lower frequency peak and the part of the curve between the peaks are much higher than those of the experimental curve. A better match can be achieved (solid line) by increasing the value of internal damping of the corresponding trapped water case only by a factor of two, doubling the internal stiffness and increasing (doubling) the external damping term c_1 .

Although the match of the two RAO curves for the damage ship case is at best rough (note that the discrepancies between the theoretical and experimental RAO curves for low frequencies are probably due to experimental error since it was difficult to maintain a good wave quality for long and shallow waves; the same cannot be said for the part of the RAO curve between the peaks), the above seems to indicate that the presence of an opening through which floodwater can flow to/from the sea, not only changes internal floodwater dynamics but also introduces additional external damping. Note nevertheless that no change in the m_1 term was applied. In other words, the effect of the floodwater inflow/outflow on external ship excitation seems only to be of a viscous nature.

These results might not be surprising, having observed substantial vortex shedding activity near the damage opening during the experiments. Nevertheless, it is important to point out that the above analysis quantifies (albeit roughly) for the first time the relative weight of internal and external damping excitation on a damaged ship roll motion. Furthermore, it might be worth bearing in mind

that in the foregoing the effect of floodwater mass variation terms has been totally ignored. This aspect of the problem should eventually be addressed.

5. CONCLUDING REMARKS

On the basis of the arguments presented in the foregoing the following remarks can be made:

- When floodwater is trapped inside a compartment (no inflow/outflow allowed), all of the changes observed in the behaviour of a ship are due to floodwater dynamics (internal excitation).
- Conversely, if the floodwater is allowed to flow to/from the sea through a damage opening, this will not only change floodwater dynamics significantly (and thus affect the ship response as a result of internal excitation), by also considerably affect external excitation parameters. This second effect seems to be mainly of a viscous nature.
- The values of inertial and restoring terms of the floodwater system seem to be fairly high. This seems to suggest that the assumption that floodwater can be treated as point mass should be revised.

6. ACKNOWLEDGEMENTS

Much of the work presented in this paper was conducted within the EC funded RTD project NEREUS (First Principles Design for Damage Resistance against Capsizing – Contract N° G3RD-CT 1999-00029). Acknowledgements also go to the FSG and WS Atkins teams.

7. REFERENCES

- [1] L. Letizia, P. Besse, A. Papanikolaou, P. Woodburn and A. Jasionowski: “First Principles Design for Damage Resistance against Capsize - NEREUS”, Final Report, 13 May 2003

- [2] Vassalos, D, Pawlowski, M and Turan, O: “A Theoretical Investigation on the Capsizal Resistance of Passenger/RORO Vessels and Proposal of Survival Criteria”, Final Report, The Joint North West European Project, University of Strathclyde, Department of Ship and Marine Technology, March 1996.

- [3] Jasionowski, A, Vassalos, D, Shu Hong Chai, Samalekos, P: “Time-Based Survival Criteria for Ro-Ro Vessels, Phase II”, Final Report, January 2001

- [4] P. Woodburn, L. Letizia and P. Gallagher, “Fundamentals of Damaged Ship Survivability”, RINA Transactions, June 2002.

